Finite Element Prediction and Experimental Verification of the Failure Pattern of Proximal Femur using Quantitative Computed Tomography Images

Majid Mirzaei, Saeid Samiezadeh , Abbas Khodadadi, Mohammad R. Ghazavi

Abstract—This paper presents a novel method for prediction of the mechanical behavior of proximal femur using the general framework of the quantitative computed tomography (QCT)-based finite element Analysis (FEA). A systematic imaging and modeling procedure was developed for reliable correspondence between the QCT-based FEA and the in-vitro mechanical testing. A specially-designed holding frame was used to define and maintain a unique geometrical reference system during the analysis and testing. The QCT images were directly converted into voxel-based 3D finite element models for linear and nonlinear analyses. The equivalent plastic strain and the strain energy density measures were used to identify the critical elements and predict the failure patterns. The samples were destructively tested using a specially-designed gripping fixture (with five degrees of freedom) mounted within a universal mechanical testing machine. Very good agreements were found between the experimental and the predicted failure patterns and the associated load levels.

Keywords—Bone, Osteoporosis, Noninvasive methods, Failure Analysis

I. INTRODUCTION

THE annual increasing number of hip fracture due to osteoporosis and other bone diseases has been announced as a major public health problem [1]. The important role of these fractures in reduction of the life expectancy has motivated researchers to devise noninvasive patient-specific methods for prediction of the mechanical behavior of femur. Among various analysis methods, the quantitative computed tomography (QCT)-based finite element analysis (FEA) has shown very promising results.

In this method very accurate 3D solid models of bone can be constructed directly from the QCT images. This feature, along with a pointwise assignment of the bone mineral density (BMD)-based mechanical properties, can be used to build comprehensive FE models for the analysis of the mechanical behavior of bone. This method has been used for evaluation of the strength and failure pattern of human vertebrae [2]-[5] and femur [6]-[17].

Majid Mirzaei is with the Mechanical Engineering Department, Tarbiat Modares University, Tehran, Iran. (e-mail: mmirzaei@modares.ac.ir).
Saeid Samiezadeh was with the Mechanical Engineering Department, Tarbiat Modares University, Tehran, Iran.
Abbas Khodadadi is with the Iranian Tissue Bank, Tehran University of Medical Sciences, Tehran, Iran.
Mohammad R. Ghazavi is with the Mechanical Engineering Department, Tarbiat Modares University, Tehran, Iran.

In essence, the main justification for creation of such sophisticated mathematical models is that, *once validated*, they can be used to study the behavior of samples under different loading and boundary conditions and avoid the expensive and time consuming experiments. Thus, *the validation procedure should be designed and carried out with a minimum number of complementary experiments to be cost-effective and meaningful*. Here, a main difficulty is the lack of a robust reference system for reliable correspondence between the QCT-based FEA and the in-vitro mechanical testing. This problem may cause significant errors in applying similar loading directions and boundary conditions in the FEA and the mechanical testing.

In several reported studies, the femoral *coronal plane* has been defined as the plane containing the *femoral cervical and shaft axes* and used for both modeling and mechanical testing of femur [7], [8], [12]. Nevertheless, since these femoral parts have complex geometries without any axisymmetric feature, certain ambiguities exist about *recognition* of these axes on femoral samples, particularly during the mechanical testing. Moreover, the lack of a *unique definition* of these axes for both FEA and mechanical testing can be troublesome. In the view of the above arguments, the overall objective of the current study was the implementation the QCT-voxel based FEA for prediction of the mechanical behavior of proximal femur.

The specific objectives can be summarized as

a. Design and implementation of systematic imaging and modeling procedures for reliable correspondence between the QCT-based FEA and the in-vitro mechanical testing.

b. Verification of the applicability of the proposed techniques and procedures through investigation of the fracture patters for two different samples at two different loading orientations.

II. MATERIALS AND METHODS

A. Sample Preparation

Two different femoral samples were excised from 2 cadavers (male and female, with 44 and 25 years old respectively) within 24 hours from their death. Plain radiographs of the samples were examined to ascertain the lack of metastatic diseases, pathologic defects, or insufficiency fractures.

B. Definition and Implementation of the Femoral Reference Frame

The orientations of mechanical loadings on femoral samples are usually adjusted with respect to the coronal plane, which is defined as the plane containing the *femoral cervical and shaft axes*. As mentioned before, due to the complex geometry of human femur, a unique definition and recognition of these axes on the femoral samples is very difficult, particularly during the mechanical testing. Moreover, an arbitrary *definition* of these axes for the two environments of FEA and mechanical testing can be quite troublesome. We propose a new approach in which 3 particular points are described on the femoral surface to establish a reference plane (the femoral coronal plane) using three different views (see Fig.1), i.e., the medial, the axial top, and the axial bottom views as follows:

1. The center point of the femoral head form the medial view (point 1)
2. The center point of the femoral head from the axial top view (point 2)
3. The center point of femoral shaft from the axial bottom view (point 3)

In spite of the fact that the femoral head is not quite spherical and the femoral shaft is not quite cylindrical, the three points can be defined without ambiguity as depicted in Fig. 1. In order to designate these points on the sample and use them as a unique reference system for both mechanical testing and FEA, the sample is placed in a specially-designed holding frame (see Fig.2). As depicted in Fig.2c, this frame has two side plates which move simultaneously in opposite directions using special connecting rods so that, upon contact with the femoral head, the median plane of the head coincides with the frame plane. In this position, the femur can still be rotated around the axes X and Y (see Fig.2a). The Y axis rotation is prevented using a two-pin slider which upon contact with the distal part of the femoral shaft secures that the contact segment is parallel with the frame. The X axis rotation is prevented by fixation of the point 3 with the C screw. In practice, this unique position is maintained by bringing the other two screws (A and B) into contact with the points 1 and 2 respectively, and the plates and slider are detached after the initial adjustments. In this situation, the three screws represent both the frame plane and the femoral coronal plane. The role of the forth screw is just to add extra fixity.
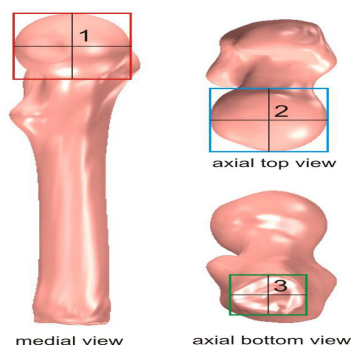

Fig. 1 Three different views of a proximal femur and the three points identified on the femoral surface for definition of the coronal plane

This reference frame remains attached to the sample during the QCT process and is naturally transferred to the 3D and the FE models. On the other hand, the role of the Plexiglas disk attached to the lower end of the distal femur is to preserve and transfer the reference system to the mechanical testing.
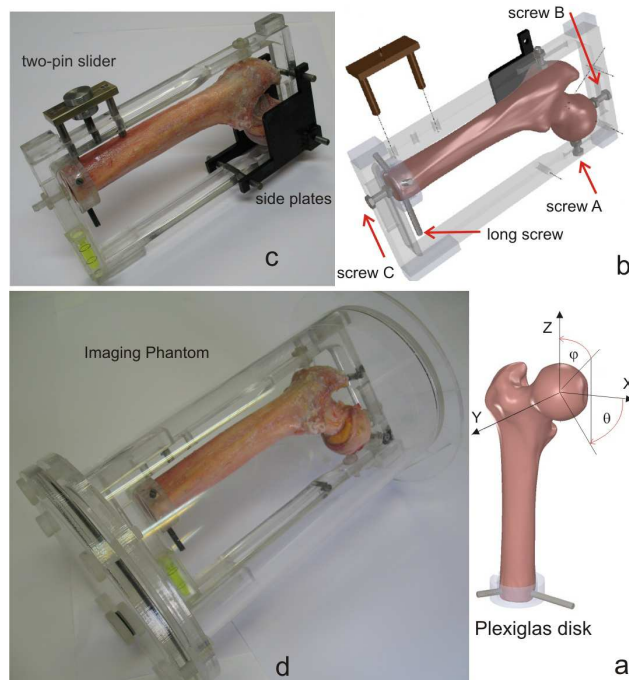

Fig. 2 (a) The spherical coordinate system on a 3D model of a sample. (b): A 3D model of the holding frame containing a sample. (c): A test sample inside the holding frame. (d): The imaging phantom containing the holding frame and a test sample

As depicted in Fig. 2, the disk has three screws which are used to bring it to the desired location and orientation with respect to both the femoral shaft and the holding frame, where it can be permanently fixed to the shaft using dental PMMA (polymethylmethacrylate). In its final position, the disk plane is parallel to the lower side of the holding frame, its axis of rotation passes through point 3, and the direction of its long screw lies in the defined coronal plane. Thus, when the femur is detached from the holding frame, the disk preserves the location and orientation of the defined coronal plane. In practice, the orientation of the femoral sample during the mechanical testing is adjusted using the attached disk. It should be mentioned that the holding frame, the screws, and the disk are all made of Plexiglas to avoid artifacts during QCT scans.

In brief, the above method for defining and maintaining a reference plane for each sample has the following advantages:

a. Both the holding frame and the disk remain attached to the femur during the QCT scanning, so the defined reference system is naturally preserved and transferred during the image processing and 3D FE modeling.

b. The lower end of the femoral shaft and the femoral coronal plane are both perpendicular to the Plexiglas disk surface,

so during the mechanical testing a complete contact between the disk and the base plate of the gripping system guarantees that both the shaft and the coronal plane are perpendicular to the base plate. Moreover, the long screw of the disk acts as an indicator for the rotation of the coronal plane around the shaft axis.

C. QCT Scanning

Each framed sample was placed inside a Plexiglas container filled with water, designed as an imaging phantom for QCT studies (Fig.2d). The QCT scans were carried out using a clinical scanner (Siemens-Somatom 64, 140 kV, 80 mAs, 0.5×0.5 mm/pixel resolution, and 1mm slice thickness). Using a calibration phantom (Mindways Software, Inc., San Francisco, CA), grayscale values were mapped to K2HPO4 equivalent density (ρ_{KHP}) using five tubes with reference densities and the Hounsfield Units (HUs) were calibrated. Fig.3 shows a view of the scanner, the imaging and calibration phantoms, and a section of a sample embedded in the imaging phantom.
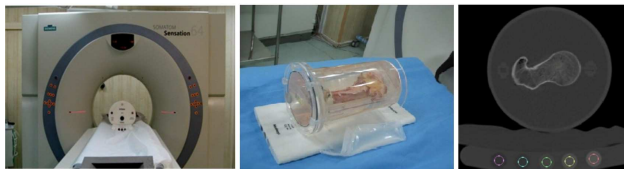

Fig. 3 The CT axial view of the scanner, the imaging and calibration phantoms, and a section of a sample embedded in the imaging phantom

D. Finite Element Analysis

The segmentation of the bone hard tissue from the surroundings was performed using the procedure described in [5]. The FE models were generated by conversion of each *voxel* into an 8-noded brick element compatible with the format of the ANSYS software (ANSYS. Inc., Canonsburg, PA) (see Fig. 4).

Fig. 4 A proximal femur sample along with its 3D solid and FE models

The ash density for each voxel was calculated from the calibrated CT scan data [18] ($\rho_{ash} = 1.22\rho_{KHP} + 0.0526$). The bone tissue was assumed as inhomogeneous isotropic material with linearly elastic properties for linear analyses and linearly elastic-perfectly plastic behavior for nonlinear analyses. Specific modulus of elasticity (*E*) and yield strength (*S*) values were assigned to *each element* using the empirical relationships based on ash density for trabecular and cortical bone [19]:

$$E = 33,900\rho_{ash}^{2.20} \quad \text{for} \quad \rho_{ash} \leq 0.27 \text{ (trabecular bone),}$$

$$E = 10,200\rho_{ash}^{2.01} \quad \text{for} \quad \rho_{ash} \geq 0.6 \quad \text{(cortical bone),}$$

$$E = 5,307\rho_{ash} + 469 \quad \text{for} \quad 0.27 < \rho_{ash} \leq 0.6 \quad \text{(transition),}$$

$$S = 137\rho_{ash}^{1.88} \quad \text{for} \quad \rho_{ash} \leq 0.317 \quad \text{(trabecular bone),}$$

$$S = 114\rho_{ash}^{1.72} \text{ for } \rho_{ash} \geq 0.317 \text{ (cortical bone).}$$

The three reference points were identified from CT scans and the coronal plane was recognized and used for application of the load and the boundary conditions.

Definition of a general coordinate system for application of mechanical loads on femur is another important issue in FEA of femoral samples [20], [7], [12], [21]. Conventionally, two angles are defined and used for loading of femur, i.e., α (the angle between the applied load and the sagittal plane) and β (the angle between the load and the coronal plane) [7]. In this study, we defined a spherical coordinate system on the femoral head as depicted in Fig. 2a. Table I shows the loading orientations in the conventional α-β and the new θ-φ systems.

TABLE I
THE TWO LOADING ORIENTATIONS FOR THE TWO STANCE CONFIGURATIONS (SC1 AND SC2) USED IN THIS STUDY.

	α(°)	β(°)	θ(°)	φ(°)
SC1	15	0	0	15
SC2	20	20	45	27

All the nodes on the surface of the femoral head were identified and the load was distributed among the nodes located on a 30mm-diameter cap (the contact surface of the steel cap used in the mechanical testing) in the desired direction. The nodes on the clamped cross section of the shaft were fully restrained [7]. The FE models of the two samples consisted of approximately 190,000 brick elements. All elements with the modulus below 5 MPa were assigned a low modulus of 0.01 MPa [6]. The elements loaded on the femoral head were identified and assigned an elastic modulus of 20 GPa and a yield strength of 200 MPa to prevent element distortion [8]. The Poisson's ratio was assumed 0.4 [6].

The equivalent plastic strains obtained from the nonlinear analyses were used to predict the occurrence of local failures and development of the failure patterns. In the linear analyses, the strain energy density measure was used to identify the critical elements and predict the failure patterns.

E. Mechanical Testing

The mechanical tests were conducted using a mechanical loading frame (INSTRON Corporation, Canton, MA). The samples were destructively tested using a specially-designed gripping fixture. The fixture has five degrees of freedom and can be used to test the samples in various orientations within a

specified range (see Fig.5). The mechanical setup shown in Fig. 5 can work within the range of -30°<α<30° and -30°<β<30°, which covers almost all the physiologic and the non-physiologic axial loadings in the stance configuration. However, a mapping is required for application of these angles to the loading fixture. Fig.5 also shows a 3D model of the loading fixture mounted in the test machine. The model was created using SolidWorks (Dassault Systèmes) to map the angles in the spherical coordinate system into the adjustable angles of the fixture. Another problematic issue in the mechanical testing of femoral samples in the *slanted* directions is the slip rotation of the distal part inside the grip. On the other hand, the usage of rough grip faces and application of high gripping forces can damage the sample. In our experiments, the distal diaphysis (length of 85 mm) was mounted within a steel sleeve filled with PMMA, and a steel pin was inserted through the whole assembly as shown in Fig. 5. The outer surface of the sleeve has three grooves that match the three sliding faces of the gripping fixture and thereby the slip rotation is prevented without damaging the sample. The final step is the adjustment of the sample to ensure that the bottom surface of the Plexiglas disk is in full contact with the gripping base, and the orientation of its long screw coincides with the reference plane of the fixture.
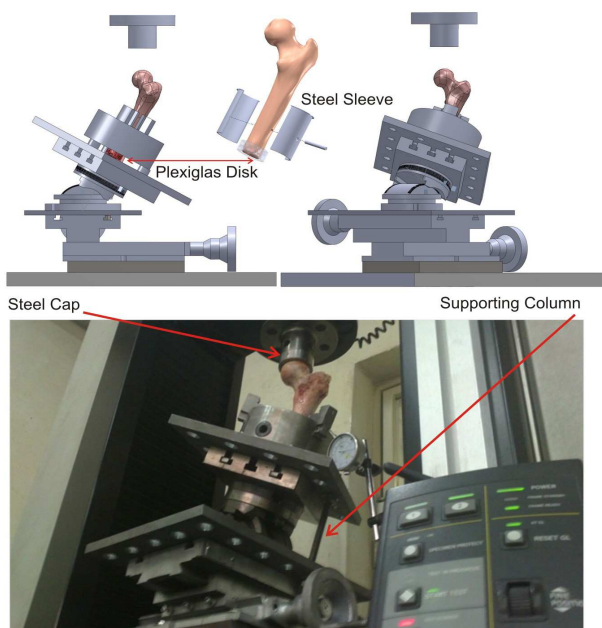

Fig. 5 Top: Schematic of a sample prepared for mechanical testing along with the gripping fixture. Bottom: the gripping fixture mounted within the mechanical testing machine

In this position, the coronal plane of the sample and the reference plane of the fixture coincide (see Fig. 5).

We also used specially-designed steel caps for uniform distribution of compressive force on the femoral head (see Fig. 5). The size of the cap was selected based on the femoral head diameter of each sample. A preload of 100N was applied in each test and the application of the main load, at a rate of 1 mm/min, was sufficiently delayed for stabilization of both the load and displacement readings. The vertical displacement of the base plate of the fixture was measured using a dial indicator and subtracted from the readings of the total displacement.

III. RESULTS

The first set of results was obtained from nonlinear elasto-plastic large deformation analyses. The average nodal displacements of all the nodes attached to the femoral cap in each step were calculated and the load-displacement diagrams were obtained for each specimen.

Fig. 6 shows the experimental load-displacement diagrams along with the FEA results. The maximum load in these diagrams was considered as the femoral ultimate strength. The stiffness values obtained from the nonlinear analyses and the experiments were calculated from the slope of the linear part of the related diagrams (see Table II).

TABLE II
THE RESULTS OF LINEAR ANALYSES FOR STIFFNESS (S_{LFE}), AND NONLINEAR ANALYSES FOR STIFFNESS (S_{NLFE}) AND STRENGTH (F_{NLFE}), ALONG WITH THE EXPERIMENTAL STIFFNESS (S_{EXP}) AND STRENGTH (F_{EXP}) OBTAINED FOR THE TWO SAMPLES LOADED IN DIFFERENT ORIENTATIONS

Sample Loading Direction	S_{LFE} kN/mm	S_{NLFE} kN/mm	S_{EXP} kN/mm	F_{NLFE} kN	F_{EXP} kN
F1(female) SC2	2.8	2.6	2.1	8.1	7.0
F2(male) SC1	11.8	10.9	8.8	13.8	11.7

In order to track the initiation and progression of damage in the FE models the elements with nonzero equivalent plastic strain were identified in each load step and the locus of these elements was considered as the failure pattern. The predicted pattern of local failure in the first sample (F1) is shown in Fig. 7 (d, e, f), in which only the *identified elements* are shown for clarity. In this sample the initiation of local failure occurs on the femoral shaft below the lesser trochanter at a load level of 2.6 kN. By increasing the load, the yielded elements increases and form a distinct integrated damaged zone at a load level of 3.7 kN. This load level (which is much lower than the ultimate strength of 8.1 kN) can be considered as the local failure load from a practical point of view because, in practice, physicians refer to similar failed regions on the plain radiographs as fractures. The occurrence of a similar failure pattern at the same location (in the form of a distinct crack) is clearly visible on the experimental sample (see Fig.7).

The second set of FE results was obtained for the same sample from linear-elastic small-deformation analyses and the strain energy density was obtained for each element. A simple computer code was developed to sort the elemental risk factor (RF) by computing the ratio of the strain energy density to the yield strain energy density for each element. The locus of the elements with the highest RF (critical elements) was considered as the failure initiation site. The development of the failure pattern was simulated by increasing the percentage of the screened elements [5].
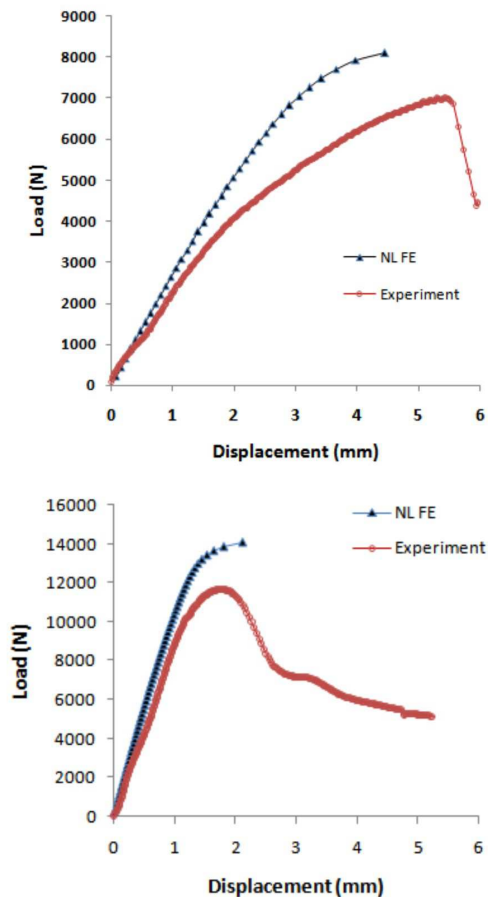
Fig. 6 The experimental and nonlinear FEA load-displacement diagrams for the two samples. Top: F1 sample. Bottom: F2 sample
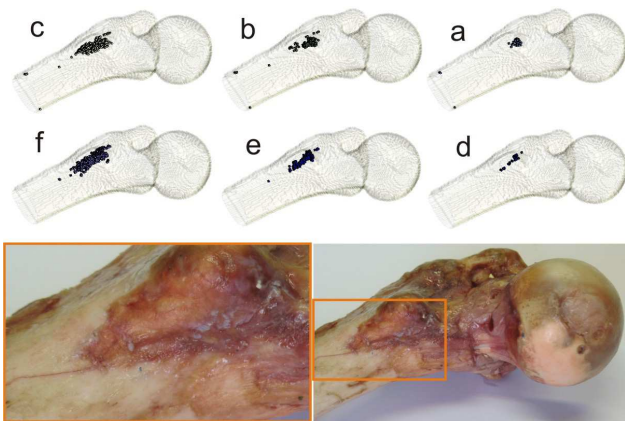

Fig. 7 Top row: predicted pattern of failure initiation and growth for the F1 sample, obtained from linear FEA. The screening percentages are: 0.02% (a), 0.09% (b), and 0.31% (c). Middle row: predicted pattern of failure initiation and growth for the same sample obtained from nonlinear FEA. Bottom row: the failure pattern of the same sample after mechanical testing

As depicted in Fig. 7 (a, b , c) the locus of the critical elements conform to the actual failure pattern of the sample. Fig. 8 shows similar comparisons for the second sample (F2) which experienced a *totally different* initiation and propagation pattern. For this sample, the initiation starts at a load level of 5.4 kN (Fig. 8d) and develops to a distinct damaged zone at a load level of 7.8 kN (Fig. 8e). The same failure pattern was predicted by the linear analysis as shown in Fig.8 (a, b, c).

IV. DISCUSSION

In general, the results of this investigation showed the robustness of the QCT voxel-based FEA in prediction of the femoral strength as well as the failure initiation and growth patterns (see TABLE II and Figs. 6-8). Nevertheless, it should be noted that the failure analysis of human femur under physiologic and non-physiologic constraints and loads is a complicated and difficult task. The stress and strain analysis of proximal femur is an integrated part of this task which requires both accuracy and precision in all the aspects of modeling such as; creation of complex geometries, assignment of linear and nonlinear heterogeneous mechanical properties, and application of loading and constraints in various 3D spatial orientations. The first two aspects can be essentially maintained due to the ability of the QCT voxel-based FEM in development of very accurate image-based 3D models of the bone geometry plus a pointwise description of BMD-based material properties. However, successful maintenance of the loading directions and boundary conditions in 3D spatial orientations require an unambiguous definition of a robust reference system which can be used in both the QCT-based FEA and the in-vitro mechanical testing. In this study a novel method was developed to establish *similitude* conditions between the two environments of FE modeling and mechanical testing through an unambiguous definition and recognition of the femoral coronal plane. The very good agreement between the predicted and experimental results obtained for two different samples (*with marked differences in size, strength, and flexibility*), *under two different loading and boundary conditions*, confirms the robustness and applicability of the proposed method.

As mentioned before, the main justification for creation of such sophisticated FE models is that, *once validated*, they can be used to study the behavior of samples under different loading and boundary conditions and avoid the expensive and time consuming experiments. Thus, the validation procedure should be designed and carried out with a minimum number of complementary experiments to be cost-effective and meaningful. We believe that the implementation of the proposed reference system and analysis procedures can reduce the number of the required experimental validation to one experiment on a single specimen loaded in an arbitrary spatial orientation. The reason is that the proposed routines are quite robust and deterministic, so there is no use for the collection of large experimental datasets which are usually gathered for statistical analyses. However, in practice we analyzed and

tested two different samples to confirm the reliability of the proposed techniques and procedures. On the other hand, it should be noted that in spite of its superior precision, the nonlinear analysis of voxel-based FE models is rather difficult, computationally expensive, and time consuming. In contrast, the linear-elastic small-deformation analysis of the same models is very fast and much easier to implement, so it is clinically more feasible. We showed that the failure pattern of femoral samples can be predicted using the strain energy density distribution with much less effort. The ability of the strain energy density measure in prediction of the failure pattern can be attributed to the micro-mechanism of local failures in bone tissue. The micro-mechanism of failure of porous trabecular tissue is mostly in the form of spicule (trabecula) buckling [22] and the failure mechanism of denser trabecular and nearly homogenous cortical tissues is mostly of the form of local cracking. In either case (buckling or cracking), the strain energy density can be considered as a viable damage controlling parameter from a solid mechanics point of view [5].
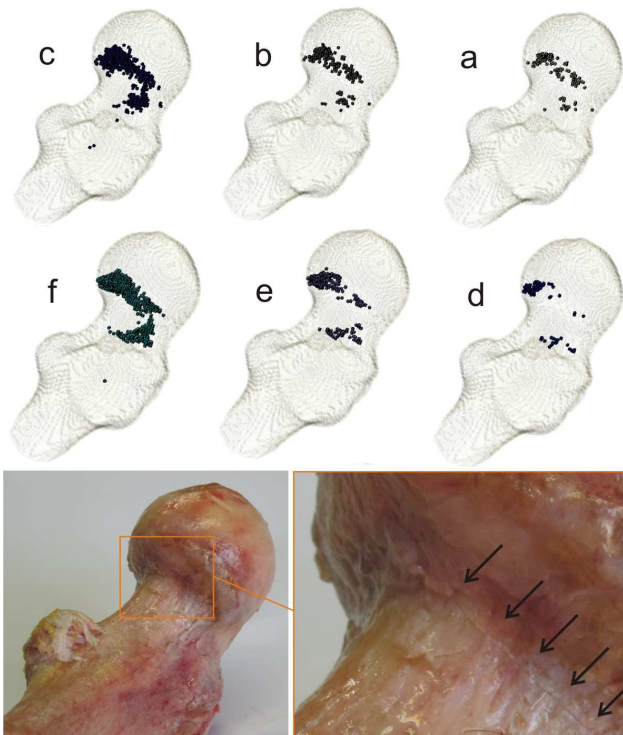

Fig. 8 Top row: predicted pattern of failure initiation and growth for the F2 sample, obtained from linear FEA. The screening percentages are: 0.06% (a), 0.11% (b), and 0.35% (c). Middle row: predicted pattern of failure initiation and growth for the same sample obtained from nonlinear FEA. Bottom row: the failure pattern of the same sample after mechanical testing.

Finally, the fact is that femurs with different geometries and densitometric heterogeneity under different loading conditions will experience different failure patterns. We believe that representative and reliable FE models of such complex samples can be created and validated using the techniques and procedure developed in this study. The calibrated FE model can be used to conduct comprehensive and reliable studies on the material assignment methods, loading conditions, and failure criteria.

REFERENCES

[1] P. Sambrook, C. Cooper, "Osteoporosis," *Lancet*, vol. 367, no. 9527, pp. 2010-2018, 2006.
[2] M.A.K. Liebschner, D.L. Kopperdahl, W.S. Rosenberg, T.M. Keaveny, "Finite element modeling of the human thoracolumbar spine," *Spine*, vol. 28, pp. 559-565, 2003.
[3] R.P. Crawford, C.E. Cann, T.M. Keaveny, "Finite element models predict in vitro vertebral body compressive strength better than quantitative computed tomography," *Bone*, vol. 33, pp. 744-750, 2003.
[4] J.M. Buckley, K. Loo, J. Motherway, "Comparison of quantitative computed tomography-based measures in predicting vertebral compressive strength," *Bone*, vol. 40, pp. 767-774, 2007.
[5] M. Mirzaei, A. Zeinali, A. Razmjoo, M. Nazemi, "On prediction of the strength levels and failure patterns of human vertebrae using quantitative computed tomography (QCT)-based finite element method," *J Biomech*, vol. 42, pp. 1584-1591, 2009.
[6] J.H. Keyak, S.A. Rossi, K.A. Jones, H.B. Skinner, "Prediction of femoral fracture load using automated finite element modeling," *J Biomech*, vol. 31, no. 2, pp. 125-133, 1998.
[7] J.H. Keyak, H.B. Skinner, J.A. Fleming, "Effect of force direction on femoral fracture load for two types of loading conditions," *J Orthop Res*, vol. 19, no. 4, pp. 539-544, 2001.
[8] J.H. Keyak, T.S. Kaneko, J. Tehranzadeh, H.B. Skinner, "Predicting proximal femoral strength using structural engineering models," *Clin Orthop Relat Res*, vol. 437, pp. 219-228, 2005.
[9] J.H. Keyak et al., "Male-female differences in the association between incident hip fracture and proximal femoral strength: A finite element analysis study," *Bone*, vol. 48, no. 6, pp. 1239-1245, 2011.
[10] D.D. Cody, G.J. Gross, F.J. Hou, H.J. Spencer, S.A. Goldstein, D.P. Fyhrie, "Femoral strength is better predicted by finite element models than QCT and DXA," *J Biomech*, vol. 32, no. 10, pp. 1013-1020, 1999.
[11] M. Bessho, I. Ohnishi, J. Matsuyama, T. Matsumoto, K. Imai, K. Nakamura, "Prediction of strength and strain of the proximal femur by a CT-based finite element method," *J Biomech*, vol. 40, no. 8, pp. 1745-1753, 2007.
[12] M. Bessho, I. Ohnishi, T. Matsumoto, S. Ohashi, J. Matsuyama, K. Tobita, M. Kaneko, K. Nakamura, "Prediction of proximal femur strength using a CT-based nonlinear finite element method: Differences in predicted fracture load and site with changing load and boundary conditions," *Bone*, vol. 45, no. 2, pp. 226-231, 2009.
[13] Z. Yosibash, N. Trabelsi, C. Milgrom, "Reliable simulations of the human proximal femur by high-order finite elements analysis validated by experimental observations," *J Biomech*, vol. 40, pp. 3688-3699, 2007.

[14] E. Schileo, F. Taddei, L. Cristofolini, M. Viceconti, "Subject-specific finite element models implementing a maximum principal strain criterion are able to estimate failure risk and fracture location on human femurs tested in vitro," *J Biomech*, vol. 41, no. 2, pp. 356-367, 2008.

[15] N. Trabelsi, Z. Yosibash, C. Milgrom, "Validation of subject-specific automated p-FE analysis of the proximal femur," *J Biomech*, vol. 42, no. 3, pp. 234-241, 2009.

[16] N. Trabelsi, Z. Yosibash, C. Wutte, P. Augat, S. Eberle, "Patient-specific finite element analysis of the human femur--A double-blinded biomechanical validation," *J Biomech*, vol. 44, no. 9, pp. 1666-21672, 2011.

[17] D. Dragomir-Daescu et al., "Robust QCT/FEA models of proximal femur stiffness and fracture load during a sideways fall on the hip," *Ann Biomed Eng*, vol. 39, no. 2, pp. 742-2755, 2011.

[18] C.M. Les, J.H. Keyak, S.M. Stover, K.T. Taylor, A.J. Kaneps, "Estimation of material properties in the equine metacarpus with use of quantitative computed tomography," *J Orthop Rest*, vol. 12, no. 6, pp. 822-833, 1994.

[19] J.H. Keyak, Y. Falkinstein, "Comparison of in situ and in vitro CT scan-based finite element model predictions of proximal femoral fracture load," *Med Eng Phys*, vol. 25, no. 9, pp. 781-787, 2003.

[20] J.H. Keyak, "Relationships between femoral fracture loads for two load configurations," *J Biomech*, vol. 33, no. 4, pp. 499-502, 2000.

[21] L. Cristofolini, G. Conti, M. Juszczyk, S. Cremonini, S.V. Sint Jan, M. Viceconti, "Structural behaviour and strain distribution of the long bones of the human lower limbs," *J Biomech*, vol. 43, pp. 826-835, 2010.

[22] J.S. Stolken, J.H. Kinney, "On the importance of geometric nonlinearity in finite element simulations of trabecular bone failure," *Bone*, vol. 33, pp. 496-504, 2003.